LNF-95/037

The KLOE Electromagnetic Calorimeter

J.L. Franzini, A. Antonelli, M. Antonelli, G. Barbiellini, M. Barone,
S. Bertolucci, C. Bini, C. Bloise, V. Bolognesi, F. Bossi, P. Campana,
F. Cervelli, R. Caloi, M. Cordelli, G. De Zorzi, G. Di Cosimo,
A. Di Domenico, O. Erriquez, A. Farilla, A. Ferrari, P. Franzini, F. Garufi,
P. Gauzzi, E. Gero, S. Giovannella, R. Haydar, M. Incagli, L. Keeble,
W. Kim, G. Lanfranchi, A. Martini, A. Martinis, S. Miscetti, F. Murtas,
A. Parri, A. Passeri, F. Scuri, E. Spiriti, L. Tortora, X.L. Wang, S. Wölfle

Nucl. Instr. & Meth. In Phys. Res. A, 360, 201-205, (1995)

Nuclear Instruments and Methods in Physics Research A 360 (1995) 201–205

ELSEVIER

NUCLEAR INSTRUMENTS & METHODS IN PHYSICS RESEARCH Section A

The KLOE electromagnetic calorimeter

Juliet Lee-Franzini [a,b,*], A. Antonelli [a], M. Antonelli [a], G. Barbiellini [g], M. Barone [a], S. Bertolucci [a], C. Bini [e], C. Bloise [a], V. Bolognesi [a], F. Bossi [a], P. Campana [a], F. Cervelli [d], R. Caloi [e], M. Cordelli [a], G. De Zorzi [e], G. Di Cosimo [e], A. Di Domenico [e], O. Erriquez [c], A. Farilla [c], A. Ferrari [d], P. Franzini [e], F. Garufi [e], P. Gauzzi [e], E. Gero [a], S. Giovannella [a], R. Haydar [a], M. Incagli [d], L. Keeble [a], W. Kim [b], G. Lanfranchi [a], A. Martini [a], A. Martinis [g], S. Miscetti [a], F. Murtas [a], A. Parri [a], A. Passeri [f], F. Scuri [g], E. Spiriti [f], L. Tortora [f], X.L. Wang [a], S. Wölfle [a]

[a] *Laboratori Nazionali di Frascati, Via Enrico Fermi 40, 00044 Frascati, Italy*
[b] *Physics Department, State University of New York at Stony Brook, Stony Brook, New York 11794, USA*
[c] *Dipartimento di Fisica dell'Università e Sezione INFN Bari, Italy*
[d] *Dipartimento di Fisica dell'Università e Sezione INFN Pisa, Italy*
[e] *Dipartimento di Fisica dell'Università e Sezione INFN Roma, Italy*
[f] *Istituto Superiore di Sanità and Sezione INFN, ISS, Roma, Italy*
[g] *Dipartimento di Fisica dell'Università Sezione INFN Trieste / Udine, Italy*

Abstract

A general purpose detector, KLOE, is under construction for operations at the Frascati ϕ factory, DAΦNE. Its central mission is the study of direct CP violation in K^0 decays, which places very stringent requirements on electromagnetic shower measurements in the 20–280 MeV/c region. We have chosen to use a lead–scintillator sampling calorimeter, EmC, consisting of very thin (0.5 mm) lead layers in which are embedded 1 mm diameter scintillating fibers. Much prototyping and testing has been done during its design, yielding, for the final EmC, an expected energy resolution of $\sigma(E)/E \sim 4.4\%/\sqrt{E(\mathrm{GeV})}$ and a time resolution of ~ 46 ps$/\sqrt{E(\mathrm{GeV})}$, with excellent linearity in the region of interest and with little dependence on incidence angle and entry position.

1. Introduction

The main goal of the KLOE [1] experiment at the DAΦNE ϕ-factory [2] in Frascati is to study CP violation in K^0 decays by measuring $R(\epsilon'/\epsilon)$ with an accuracy of $O(10^{-4})$. Since $K_{L,S}$ neutral decays ($K_{L,S} \to \pi^0\pi^0$) produce four photons between 20 and 280 MeV, identification of these decays and rejection of the $K_L \to 3\pi^0$ background [1,2] means that the electromagnetic calorimeter (EmC) plays a crucial role in this measurement. Vertex reconstruction of $K^0 \to \pi^0$'s $\to \gamma$'s in KLOE can be performed by measuring the arrival time of each photon on the calorimeter surface [3], because of the low speed of the K^0 ($\beta_K \sim 0.2$), requiring excellent timing accuracy of the EmC. In addition, the calorimeter should also provide a fast and unbiased first level trigger for the detector. Finally, it should have some particle identification capability, to aid rejection of $K_{\mu 3}$ decays. The requirements for the KLOE EmC are: a) time resolution $O(50$ ps$/\sqrt{E(\mathrm{GeV})})$, b) energy resolution $O(5\%/\sqrt{E(\mathrm{GeV})}$, c) shower vertex resolution $O(1$ cm), d) full efficiency for γ's in the energy range 20–280 MeV, and e) hermeticity.

2. The KLOE electromagnetic calorimeter design

The KLOE EmC is a very fine sampling lead–scintillating fiber calorimeter, with photomultiplier (PMs) read-out. The central part (barrel) approximates a cylindrical shell of 4 m inner diameter, 4.3 m effective length and 23 cm thickness. The barrel covers the polar angle region $49° < \theta < 131°$ and consists of 24 sectors with trapezoidal cross section, ~ 60 cm wide. Two end-caps, 4 m in diameter and 23 cm thick, close the calorimeter hermetically. Each end-cap, consists of 26 C shaped modules which run vertically along the chords of the circle inscribed in the barrel. At the two ends they are bent by 90°, becoming parallel to the barrel ends, to decrease the effects of the

* Corresponding author.

0168-9002/95/$09.50
SSDI 0168-9002(94)01607-0

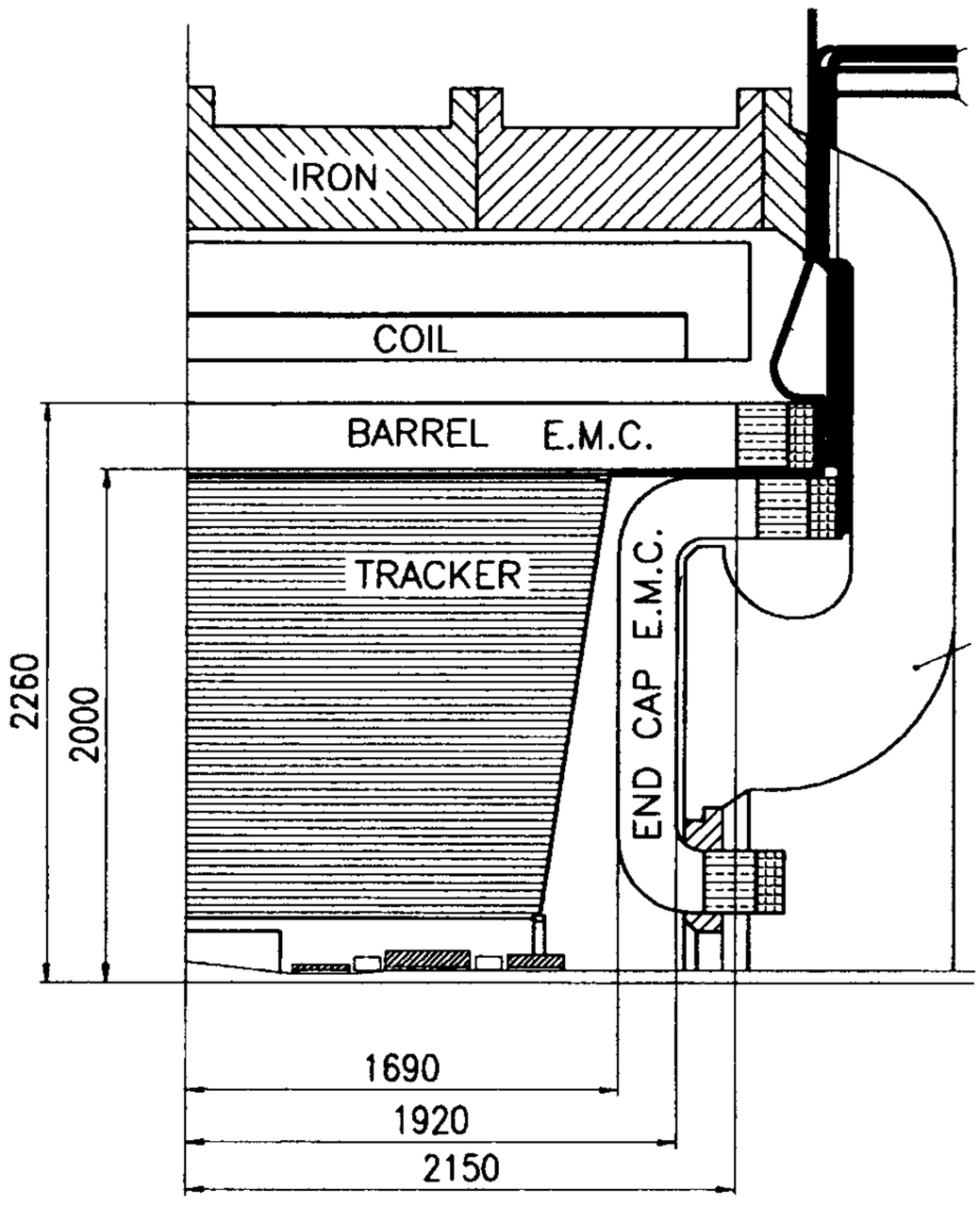

Fig. 1. Cross section of the KLOE calorimeter.

magnetic field on the PMs and to increase hermeticity. A quater cross section of the KLOE calorimeter is shown in Fig. 1. In our EmC fibers run mostly transversely to the particle trajectories. This reduces sampling fluctuations due to channeling, resulting in improved resolution particularly important at low energies.

Each module of the KLOE EmC is built by gluing 1 mm diameter blue scintillating fibers between thin grooved lead plates, obtained by passing 0.5 mm thick lead foils through rollers of a proper shape. The grooves in the two sides of the lead are displaced by one half of the pitch so that fibers are located at the corners of adjacent, quasi-equilateral triangles resulting in optimal uniformity of the final stack. The grooves are just big enough to insure that the lead does not apply direct pressure on the fibers. Light travelling in the cladding is effectively removed because of the glue surrounding the fibers. The selected fiber pitch of 1.35 mm results in a structure which has a fiber:lead:glue volume ratio of 48:42:10 and a sampling fraction of $\sim 15\%$ for a minimum ionizing particle. The final composite has a density of ~ 5 g/cm^3 and a radiation length X_0 of ~ 1.6 cm, is self-supporting and can be easily machined. The very small lead foil thickness ($< 0.1 X_0$) results in a quasi-homogeneous structure and in high efficiency for low energy photons. Measurements indicate that the blue–green Kuraray SCSF-81, Bicron BCF-12 and Pol.Hi.Tech-46 fibers satisfy our requirements for light yield, scintillation decay time and attenuation length [4]. Since the time resolution depends on the light yield, great care has been taken to maximize the efficiency of the light collection system and insure uniform photocathode illumination. Each light guide consists of a mixing part and a Winston cone concentrator [5]. We are thus able to match the calorimeter elements to the PM photocathodes, with an area reduction factor of up to ~ 4, without losses, because of the small divergence angle (22°) of the light travelling in the fibers.

3. Prototype tests

We built a barrel prototype module of dimensions $14 \times 24 \times 203$ cm^3. The module depth of 24 cm is equivalent to a thickness of $15 X_0$. The calorimeter consists of 207 lead and scintillating fiber layers for a grand total of 21 450 fibers and a weight of 330 kg. A prototype module for the end-cap region, consisting of two C shaped modules, was also built. The width of each module is 7 cm and they both have the same depth of 24 cm. Each section consists of a central straight piece (89 and 110 cm), two curved pieces with an inner radius of 7.5 cm, and two straight end pieces to which light guides are glued. The readout, identical for both modules, was organized into 22 elements for each side: five planes of four small elements, 3.5×3.5 cm^2, and two large rear elements, 6.5×7 cm^2. The small elements on each side are viewed by $1\frac{1}{8}$ in. diameter PMs, with an area concentration factor of ~ 2.7. The rear was viewed by 5 cm diameter PMs, with an area concentration factor of ~ 2.5.

The calorimeter prototypes have been tested [6] at the Paul Scherrer Institut (PSI) in Villigen, Switzerland. The PSI machine is an isochronous cyclotron which accelerates protons to 600 MeV kinetic energy. A secondary beam of π's, μ's and e's in the momentum range 50–400 MeV/c was delivered to the test areas. Two crossed scintillators in front of the calorimeter and a third counter, 4.5 m away from the calorimeter, provided a beam trigger, defined the beam position at the calorimeter and enabled $\pi/\mu/e$ identification by time of flight. The barrel prototype has also been tested with tagged low energy photons (20–80 MeV) at the Frascati LADON facility [7]. The trigger was obtained by a coincidence from the two calorimeter ends, after adding all signals from each side.

4. Energy response and resolution

In the following the z-axis is along the module axis. In the analysis of the energy response of the modules we define the total visible energy E_{vis} as the sum over all elements read out on both ends, labelled A and B. The the signal $E_{\mathrm{adc},i}$ of channel i, is divided by the calibration constants $K_{\mathrm{mip},i}$:

$$E_{\mathrm{vis}} = \sum_{i=1}^{N} \frac{1}{2}(E_{\mathrm{A},i} + E_{\mathrm{B},i}) \quad \text{with} \quad E_i = \frac{E_{\mathrm{adc},i}}{K_{\mathrm{mip},i}}. \qquad (1)$$

The calibration constants K_{mip} were obtained with cosmic rays and 400 MeV/c pions, incident at the center of each element. We define 1 mip as the visible energy deposited by a minimum ionizing particle in a 3.5×3.5 cm^2 readout element; our simulation [8] determines 1 mip to be equivalent to an average energy deposit of 3.24 MeV in the active material. Pions of 400 MeV/c momentum are minimum ionizing particles to a reasonable approximation only in the first plane of the calorimeter. We have therefore corrected for the increase of the specific ionization with calorimeter depth and for straggling effects. The energy loss from the beam passing through the trigger counters and the iron skin of the calorimeter is equivalent to 3.6 cm of scintillator and was appropriately taken into account.

The following results were obtained for positrons and photons entering the center of the calorimeter front face ($z = 0$ cm). The average calorimeter response E_{vis} versus kinetic energy for photon and positron show excellent linearity (see Fig. 2). In the same plot we have also added data for the end-cap prototype exposed to positrons (triangle symbols). The energy resolution found for positrons is $\sigma_E/E = (4.47 \pm 0.02)\%/\sqrt{E(\mathrm{GeV})}$ and for photons $\sigma_E/E = (4.35 \pm 0.01)\%/\sqrt{E(\mathrm{GeV})}$. Both e^+ and γ data are plotted together in Fig. 3. The $1/\sqrt{E}$ dependence indicates that sampling fluctuations and photoelectron statistics determine the resolution, as expected from the light yield. A similar analysis for the end-cap gives an energy resolution of $\sigma_E/E = (4.59 \pm 0.04)\%\sqrt{E(\mathrm{GeV})}$.

The response for muons and pions in the momentum range 150–280 MeV/c, corresponding to a kinetic energy of 50–180 MeV, has also been studied. The response for muons and pions is identical, with a resolution of

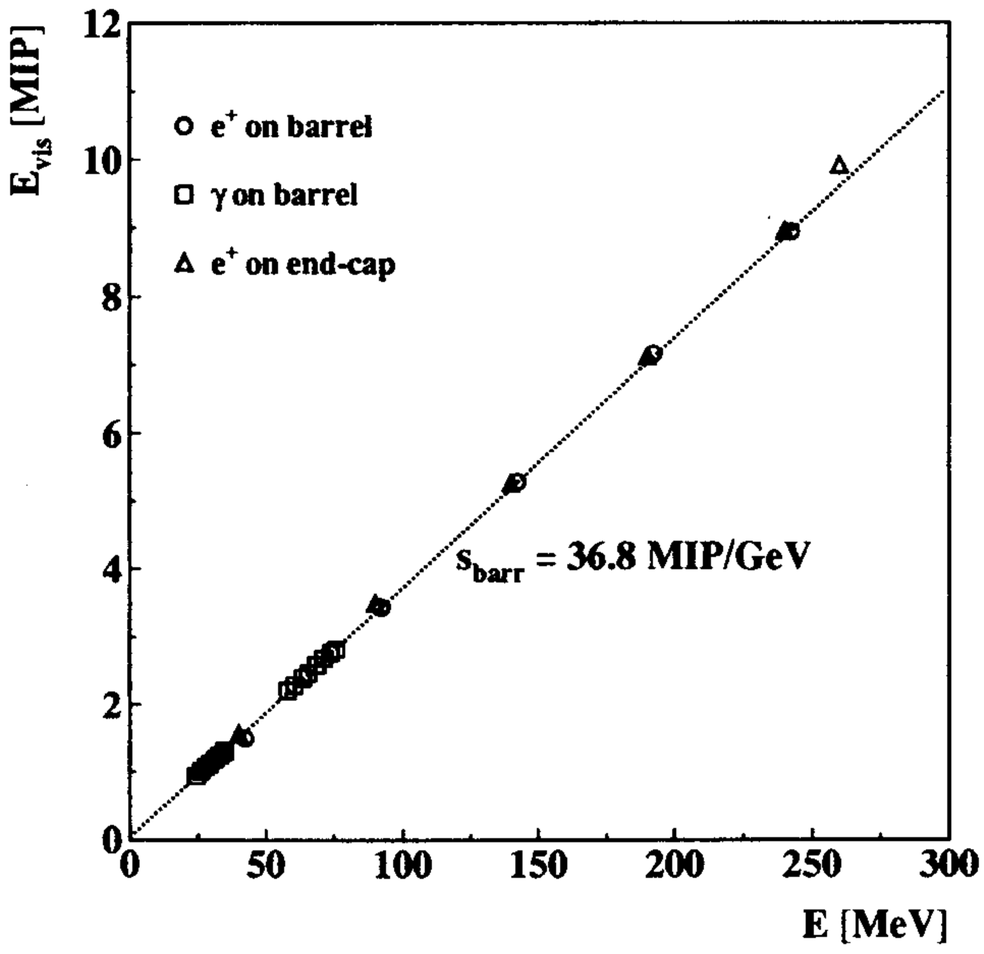

Fig. 2. Energy response for photons and positrons vs. kinetic energy.

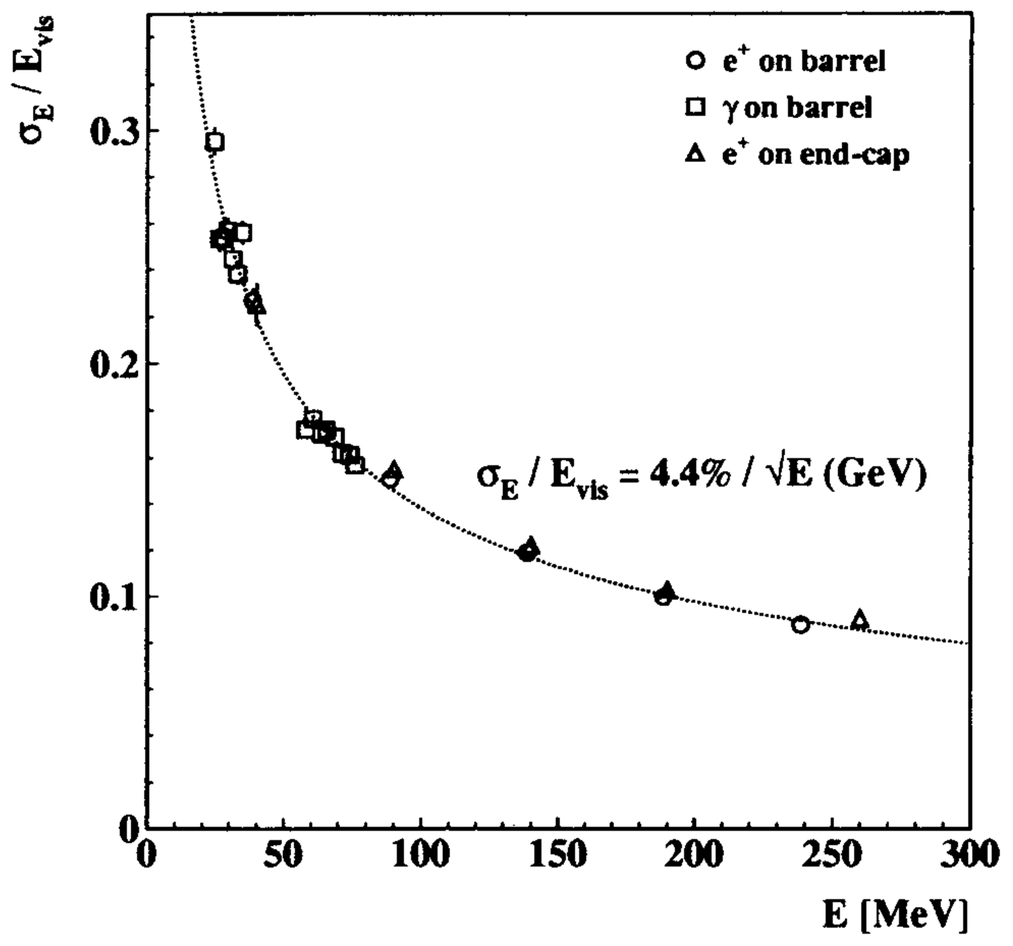

Fig. 3. Energy resolution for photons and positrons vs. kinetic energy.

$3.7\%/\sqrt{E}$. A z-scan along the module axis was performed with 200 MeV/c positrons at seven different z-positions from -80 to $+80$ cm. The z dependence of the signal is well represented as $E_{vis}(z) = E_{vis}(0)\cosh(z/\lambda)$, due to adding two exponentials, with an attenuation length $\lambda = 240$ cm, while the resolution is constant.

The response of the barrel prototype as a function of the incidence angle, θ, has been studied using photons, positrons and muons at 30°, 45° and 60° incidence. Response and resolution do not depend on θ as expected for a quasi-homogeneous calorimeter with very thin converter layers. For low energy photons, $E < 60$ MeV, we observe a small worsening of the resolution, $\sim 25\%$, at $\theta = 60°$. The curved parts of the end-cap prototype have been investigated by scanning the prototype with 200 MeV positrons incident at 45° at different positions, moving along the outer surface of the bent part. No appreciable variation was found in the scan.

5. Time resolution

The particle arrival time in the calorimeter is given, for each PM, by a discriminator output, used as a TDC "stop". For charged particles, the common "start" of the TDC system was obtained from the beam defining counters. For photons we self-triggered on the analog sum of all calorimeter signals, as mentioned previously. Time walk correction depending on pulse height were applied off-line. The times measured at each calorimeter end T_A, T_B are obtained by the energy weighted average over all elements:

$$T_A = \frac{\sum_i E_{A,i} T_{A,i}}{\sum_i E_{A_i}}; \qquad T_B = \frac{\sum_i E_{B,i} T_{B,i}}{\sum_i E_{B_i}}. \tag{2}$$

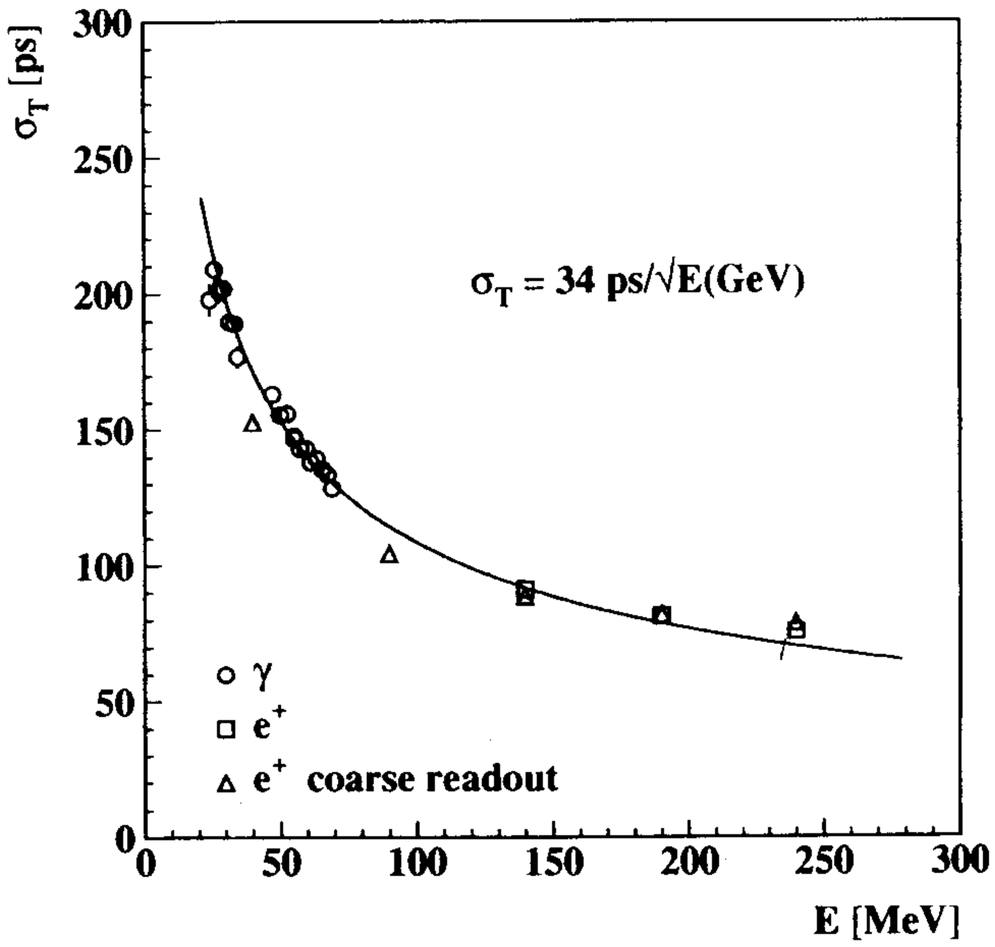

Fig. 4. Time resolution vs. energy.

The average of T_A and T_B then defines the mean arrival time T. For photons we perform our analysis in terms of the time difference

$$\Delta T = \frac{1}{2}\frac{\sum_i E_i (T_{A,i} - T_{B,i})}{\sum_i E_i}; \qquad (3)$$

ΔT and T are the difference and sum of T_A and T_B and therefore have the same rms spreads, i.e. $\sigma_{\Delta T} = \sigma_T$ except for the fact that the ''start'' time jitter is cancelled event by event in ΔT while it has to be unfolded for the external trigger case.

The dependence of $\sigma_{\Delta T}$ on beam energy for 20–80 MeV γ's and of σ_T for 50–250 MeV positrons, at normal incidence on the calorimeter surface, are shown together in Fig. 4, corresponding to a time resolution of $\sigma(T$ or $\Delta T) = 34$ ps$/\sqrt{E(\mathrm{GeV})}$. Fitting all measurements of $\sigma_{\Delta T}$ from 20 to 250 MeV gives $\sigma_{\Delta T} = 36$ ps$/\sqrt{E(\mathrm{GeV})}$, in excellent agreement with the result requiring unfolding of the ''start'' uncertainty. The measurements of the time resolution with a coarser readout granularity, (4.2×4.2 instead of 3.5×3.5 cm^2) triangle symbols in Fig. 4, are indistinguishable although the light guides area reduction factor increases from 2.7 to 3.8, showing that light collection efficiency is unchanged. For the end-cap prototype we find a time resolution of $\sigma_T = 40$ ps$/\sqrt{E(\mathrm{GeV})}$, with 50–200 MeV positrons.

The dependence of σ_T on θ was studied for all available beam energies. At 60° the resolution for 250 MeV positrons is $\sim 25\%$ worse than the result for normal incidence. The distributions are still Gaussian. At lower energies the angular dependence of the resolution becomes negligible, being dominated by sampling fluctuations. The investigation of the curved portion of the end-cap prototype as described found no dependence; only for the most extreme conditions, when the shower effectively crosses the fibers twice, the time resolution deteriorates by $\sim 20\%$.

All our measurements confirm that the time resolution scales as the number of photons to the $-1/2$ power. We therefore expect that the resolution is best at the center of the calorimeter. The z dependence of the time resolution is given by: $\sigma_T(z) = \sigma_T(0)\sqrt{\cosh(z/\lambda)}$. This has been verified with the data from the z-scan. The resolution at the two ends of the barrel module is ~ 1.05 times worse than at the center.

The z-coordinate of the entry point z_e obtained from the time difference ΔT and the effective light propagation speed in the fibers v_f is: $z_e = v_f \Delta T$. From a fit of our z-scan data we obtain $v_f = 17.2$ cm/ns, in agreement with the refractive index of the fiber core, $n = 1.6$, and the bounce angle in the fiber. The position resolution σ_z, given by $\sigma_z = v_f \sigma_{\Delta T}$, therefore is $\sigma_z = 6$ mm$/\sqrt{E(\mathrm{GeV})}$ for the electromagnetic showers.

6. Particle identification

The $K_L \to \pi\mu\nu$ decay, $K_{\mu 3}$, constitutes the most significant background to the identification of $K_L \to \pi^+\pi^-$ decays. The calorimeter can provide some π/μ identification to improve the background rejection from kinematics. [9] π/μ identification can be obtained by time of flight; Monte Carlo studies [3] show that the time resolution of the KLOE calorimeter, combined with tracking information, result in a $K_{\mu 3}$ rejection factors of 5–6, with 93% signal efficiency. π/μ identification can be achieved by studying the energy signals and the first and second moments of the energy deposition distributions. This method has been tested with data collected for pions and muons of 200–250 MeV/c; a $K_{\mu 3}$ rejection factor of 5 for is obtained while maintaining an efficiency of 95% for pions.

7. Conclusions

We have extensively tested prototypes of the KLOE calorimeter elements. Extrapolating the results described to a full length module of the KLOE calorimeter we expect:

$\sigma_E/E \sim 4.5\%/\sqrt{E(\mathrm{GeV})}$,

$\sigma_T \sim 46\mathrm{ps}/\sqrt{E(\mathrm{GeV})}$.

All results satisfy, with some safety margins, the requirements of the KLOE experiment.

References

[1] The KLOE Collaboration, A General Purpose Detector for DAΦNE, LNF-92/019 (1992).
[2] G. Vignola, Proc. 24th Int. Conf. on High Energy Physics, ed. J. Sanford (AIP, 1992) p. 1941.

[3] The KLOE Collaboration, The KLOE Detector, Technical Proposal, LNF-93/002 (1993).
[4] G. de Zorzi, Proc. 4th Int. Conf. on Calorimetry in High Energy Physics, La Biodola, Italy, 1993.
[5] H. Hinterberger and R. Winston, Rev. Sci. Instr. 37 (1966) 1094.
[6] S. Miscetti, Proc. 4th Int. Conf. on Calorimetry in High Energy Physics, La Biodola, Italy, 1993.
[7] D. Babusci et al., Nucl. Instr. and Meth. A 305 (1991) 19.
[8] S. Miscetti and A. Parri, KLOE note 111 (1994), unpublished.
[9] The KLOE Collaboration, The KLOE Central Drift Chamber, LNF-94/028 (1994).